

Measurement of exclusive $B \rightarrow X_u \ell \nu$ decays using full-reconstruction tagging at Belle

I. Adachi,¹⁰ H. Aihara,⁵¹ D. Anipko,¹ K. Arinstein,¹ T. Aso,⁵⁵ V. Aulchenko,¹
T. Aushev,^{22,16} T. Aziz,⁴⁷ S. Bahinipati,³ A. M. Bakich,⁴⁶ V. Balagura,¹⁶ Y. Ban,³⁸
E. Barberio,²⁵ A. Bay,²² I. Bedny,¹ K. Belous,¹⁵ V. Bhardwaj,³⁷ U. Bitenc,¹⁷ S. Blyth,²⁹
A. Bondar,¹ A. Bozek,³¹ M. Bračko,^{24,17} J. Brodzicka,^{10,31} T. E. Browder,⁹ M.-C. Chang,⁴
P. Chang,³⁰ Y.-W. Chang,³⁰ Y. Chao,³⁰ A. Chen,²⁸ K.-F. Chen,³⁰ B. G. Cheon,⁸
C.-C. Chiang,³⁰ R. Chistov,¹⁶ I.-S. Cho,⁵⁷ S.-K. Choi,⁷ Y. Choi,⁴⁵ Y. K. Choi,⁴⁵ S. Cole,⁴⁶
J. Dalseno,¹⁰ M. Danilov,¹⁶ A. Das,⁴⁷ M. Dash,⁵⁶ A. Drutskoy,³ W. Dungel,¹⁴ S. Eidelman,¹
D. Epifanov,¹ S. Esen,³ S. Fratina,¹⁷ H. Fujii,¹⁰ M. Fujikawa,²⁷ N. Gabyshev,¹
A. Garmash,³⁹ P. Goldenzweig,³ B. Golob,^{23,17} M. Grosse Perdekamp,^{12,40} H. Guler,⁹
H. Guo,⁴² H. Ha,¹⁹ J. Haba,¹⁰ K. Hara,²⁶ T. Hara,³⁶ Y. Hasegawa,⁴⁴ N. C. Hastings,⁵¹
K. Hayasaka,²⁶ H. Hayashii,²⁷ M. Hazumi,¹⁰ D. Heffernan,³⁶ T. Higuchi,¹⁰ H. Hödlmoser,⁹
T. Hokuue,²⁶ Y. Horii,⁵⁰ Y. Hoshi,⁴⁹ K. Hoshina,⁵⁴ W.-S. Hou,³⁰ Y. B. Hsiung,³⁰
H. J. Hyun,²¹ Y. Igarashi,¹⁰ T. Iijima,²⁶ K. Ikado,²⁶ K. Inami,²⁶ A. Ishikawa,⁴¹ H. Ishino,⁵²
R. Itoh,¹⁰ M. Iwabuchi,⁶ M. Iwasaki,⁵¹ Y. Iwasaki,¹⁰ C. Jacoby,²² N. J. Joshi,⁴⁷ M. Kaga,²⁶
D. H. Kah,²¹ H. Kaji,²⁶ H. Kakuno,⁵¹ J. H. Kang,⁵⁷ P. Kapusta,³¹ S. U. Kataoka,²⁷
N. Katayama,¹⁰ H. Kawai,² T. Kawasaki,³³ A. Kibayashi,¹⁰ H. Kichimi,¹⁰ H. J. Kim,²¹
H. O. Kim,²¹ J. H. Kim,⁴⁵ S. K. Kim,⁴³ Y. I. Kim,²¹ Y. J. Kim,⁶ K. Kinoshita,³
S. Korpar,^{24,17} Y. Kozakai,²⁶ P. Križan,^{23,17} P. Krokovny,¹⁰ R. Kumar,³⁷ E. Kurihara,²
Y. Kuroki,³⁶ A. Kuzmin,¹ Y.-J. Kwon,⁵⁷ S.-H. Kyeong,⁵⁷ J. S. Lange,⁵ G. Leder,¹⁴
J. Lee,⁴³ J. S. Lee,⁴⁵ M. J. Lee,⁴³ S. E. Lee,⁴³ T. Lesiak,³¹ J. Li,⁹ A. Limosani,²⁵
S.-W. Lin,³⁰ C. Liu,⁴² Y. Liu,⁶ D. Liventsev,¹⁶ J. MacNaughton,¹⁰ F. Mandl,¹⁴
D. Marlow,³⁹ T. Matsumura,²⁶ A. Matyja,³¹ S. McOnie,⁴⁶ T. Medvedeva,¹⁶ Y. Mikami,⁵⁰
K. Miyabayashi,²⁷ H. Miyata,³³ Y. Miyazaki,²⁶ R. Mizuk,¹⁶ G. R. Moloney,²⁵ T. Mori,²⁶
T. Nagamine,⁵⁰ Y. Nagasaka,¹¹ Y. Nakahama,⁵¹ I. Nakamura,¹⁰ E. Nakano,³⁵ M. Nakao,¹⁰
H. Nakayama,⁵¹ H. Nakazawa,²⁸ Z. Natkaniec,³¹ K. Neichi,⁴⁹ S. Nishida,¹⁰ K. Nishimura,⁹
Y. Nishio,²⁶ I. Nishizawa,⁵³ O. Nitoh,⁵⁴ S. Noguchi,²⁷ T. Nozaki,¹⁰ A. Ogawa,⁴⁰ S. Ogawa,⁴⁸
T. Ohshima,²⁶ S. Okuno,¹⁸ S. L. Olsen,^{9,13} S. Ono,⁵² W. Ostrowicz,³¹ H. Ozaki,¹⁰
P. Pakhlov,¹⁶ G. Pakhlova,¹⁶ H. Palka,³¹ C. W. Park,⁴⁵ H. Park,²¹ H. K. Park,²¹
K. S. Park,⁴⁵ N. Parslow,⁴⁶ L. S. Peak,⁴⁶ M. Pernicka,¹⁴ R. Pestotnik,¹⁷ M. Peters,⁹
L. E. Piilonen,⁵⁶ A. Poluektov,¹ J. Rorie,⁹ M. Rozanska,³¹ H. Sahoo,⁹ Y. Sakai,¹⁰
N. Sasao,²⁰ K. Sayeed,³ T. Schietinger,²² O. Schneider,²² P. Schönmeier,⁵⁰ J. Schümann,¹⁰
C. Schwanda,¹⁴ A. J. Schwartz,³ R. Seidl,^{12,40} A. Sekiya,²⁷ K. Senyo,²⁶ M. E. Sevir,²⁵
L. Shang,¹³ M. Shapkin,¹⁵ V. Shebalin,¹ C. P. Shen,⁹ H. Shibuya,⁴⁸ S. Shinomiya,³⁶
J.-G. Shiu,³⁰ B. Shwartz,¹ V. Sidorov,¹ J. B. Singh,³⁷ A. Sokolov,¹⁵ A. Somov,³ S. Stanič,³⁴
M. Starič,¹⁷ J. Stypula,³¹ A. Sugiyama,⁴¹ K. Sumisawa,¹⁰ T. Sumiyoshi,⁵³ S. Suzuki,⁴¹
S. Y. Suzuki,¹⁰ O. Tajima,¹⁰ F. Takasaki,¹⁰ K. Tamai,¹⁰ N. Tamura,³³ M. Tanaka,¹⁰
N. Taniguchi,²⁰ G. N. Taylor,²⁵ Y. Teramoto,³⁵ I. Tikhomirov,¹⁶ K. Trabelsi,¹⁰
Y. F. Tse,²⁵ T. Tsuboyama,¹⁰ Y. Uchida,⁶ S. Uehara,¹⁰ Y. Ueki,⁵³ K. Ueno,³⁰
T. Uglov,¹⁶ Y. Unno,⁸ S. Uno,¹⁰ P. Urquijo,²⁵ Y. Ushiroda,¹⁰ Y. Usov,¹ G. Varner,⁹

K. E. Varvell,⁴⁶ K. Vervink,²² S. Villa,²² A. Vinokurova,¹ C. C. Wang,³⁰ C. H. Wang,²⁹
J. Wang,³⁸ M.-Z. Wang,³⁰ P. Wang,¹³ X. L. Wang,¹³ M. Watanabe,³³ Y. Watanabe,¹⁸
R. Wedd,²⁵ J.-T. Wei,³⁰ J. Wicht,¹⁰ L. Widhalm,¹⁴ J. Wiechczynski,³¹ E. Won,¹⁹
B. D. Yabsley,⁴⁶ A. Yamaguchi,⁵⁰ H. Yamamoto,⁵⁰ M. Yamaoka,²⁶ Y. Yamashita,³²
M. Yamauchi,¹⁰ C. Z. Yuan,¹³ Y. Yusa,⁵⁶ C. C. Zhang,¹³ L. M. Zhang,⁴² Z. P. Zhang,⁴²
V. Zhilich,¹ V. Zhulanov,¹ T. Zivko,¹⁷ A. Zupanc,¹⁷ N. Zwahlen,²² and O. Zyukova¹

(The Belle Collaboration)

¹*Budker Institute of Nuclear Physics, Novosibirsk*

²*Chiba University, Chiba*

³*University of Cincinnati, Cincinnati, Ohio 45221*

⁴*Department of Physics, Fu Jen Catholic University, Taipei*

⁵*Justus-Liebig-Universität Gießen, Gießen*

⁶*The Graduate University for Advanced Studies, Hayama*

⁷*Gyeongsang National University, Chinju*

⁸*Hanyang University, Seoul*

⁹*University of Hawaii, Honolulu, Hawaii 96822*

¹⁰*High Energy Accelerator Research Organization (KEK), Tsukuba*

¹¹*Hiroshima Institute of Technology, Hiroshima*

¹²*University of Illinois at Urbana-Champaign, Urbana, Illinois 61801*

¹³*Institute of High Energy Physics,*

Chinese Academy of Sciences, Beijing

¹⁴*Institute of High Energy Physics, Vienna*

¹⁵*Institute of High Energy Physics, Protvino*

¹⁶*Institute for Theoretical and Experimental Physics, Moscow*

¹⁷*J. Stefan Institute, Ljubljana*

¹⁸*Kanagawa University, Yokohama*

¹⁹*Korea University, Seoul*

²⁰*Kyoto University, Kyoto*

²¹*Kyungpook National University, Taegu*

²²*École Polytechnique Fédérale de Lausanne (EPFL), Lausanne*

²³*Faculty of Mathematics and Physics, University of Ljubljana, Ljubljana*

²⁴*University of Maribor, Maribor*

²⁵*University of Melbourne, School of Physics, Victoria 3010*

²⁶*Nagoya University, Nagoya*

²⁷*Nara Women's University, Nara*

²⁸*National Central University, Chung-li*

²⁹*National United University, Miao Li*

³⁰*Department of Physics, National Taiwan University, Taipei*

³¹*H. Niewodniczanski Institute of Nuclear Physics, Krakow*

³²*Nippon Dental University, Niigata*

³³*Niigata University, Niigata*

³⁴*University of Nova Gorica, Nova Gorica*

³⁵*Osaka City University, Osaka*

³⁶*Osaka University, Osaka*

³⁷*Panjab University, Chandigarh*

³⁸*Peking University, Beijing*

- ³⁹*Princeton University, Princeton, New Jersey 08544*
⁴⁰*RIKEN BNL Research Center, Upton, New York 11973*
⁴¹*Saga University, Saga*
⁴²*University of Science and Technology of China, Hefei*
⁴³*Seoul National University, Seoul*
⁴⁴*Shinshu University, Nagano*
⁴⁵*Sungkyunkwan University, Suwon*
⁴⁶*University of Sydney, Sydney, New South Wales*
⁴⁷*Tata Institute of Fundamental Research, Mumbai*
⁴⁸*Toho University, Funabashi*
⁴⁹*Tohoku Gakuin University, Tagajo*
⁵⁰*Tohoku University, Sendai*
⁵¹*Department of Physics, University of Tokyo, Tokyo*
⁵²*Tokyo Institute of Technology, Tokyo*
⁵³*Tokyo Metropolitan University, Tokyo*
⁵⁴*Tokyo University of Agriculture and Technology, Tokyo*
⁵⁵*Toyama National College of Maritime Technology, Toyama*
⁵⁶*Virginia Polytechnic Institute and State University, Blacksburg, Virginia 24061*
⁵⁷*Yonsei University, Seoul*

Abstract

We report on a study of the branching fractions for the exclusive charmless semileptonic B decay modes $B \rightarrow \pi^+ \ell \nu$, $B \rightarrow \pi^0 \ell \nu$, $B \rightarrow \rho^+ \ell \nu$, $B \rightarrow \rho^0 \ell \nu$ and $B \rightarrow \omega \ell \nu$, using events tagged by fully reconstructing one of the B mesons in a hadronic decay mode. The obtained branching fractions are $\mathcal{B}(B \rightarrow \pi^+ \ell \nu) = (1.12 \pm 0.18 \pm 0.05) \times 10^{-4}$, $\mathcal{B}(B \rightarrow \pi^0 \ell \nu) = (0.66 \pm 0.12 \pm 0.03) \times 10^{-4}$, $\mathcal{B}(B \rightarrow \rho^+ \ell \nu) = (2.56 \pm 0.46 \pm 0.12) \times 10^{-4}$, $\mathcal{B}(B \rightarrow \rho^0 \ell \nu) = (1.80 \pm 0.23 \pm 0.07) \times 10^{-4}$ and $\mathcal{B}(B \rightarrow \omega \ell \nu) = (1.19 \pm 0.32 \pm 0.05) \times 10^{-4}$, where the first error in each case is statistical and the second systematic. Combining the charged and neutral pion modes using isospin invariance, the branching fraction obtained is $\mathcal{B}(B \rightarrow \pi \ell \nu) = (1.13 \pm 0.14 \pm 0.06) \times 10^{-4}$. The partial branching fractions as a function of q^2 are extracted using three q^2 bins. At low q^2 , the combined charged and neutral pion branching fractions and a Light Cone Sum Rules prescription imply $|V_{ub}| = (3.1 \pm 0.2 \pm 0.1_{-0.3}^{+0.5}) \times 10^{-3}$, while using the high q^2 data and two different lattice prescriptions implies $|V_{ub}| = (3.1 \pm 0.3 \pm 0.1_{-0.4}^{+0.6}) \times 10^{-3}$ (HPQCD) and $|V_{ub}| = (3.3 \pm 0.4 \pm 0.1_{-0.4}^{+0.6}) \times 10^{-3}$ (FNAL) respectively. In each case the errors are statistical, systematic and theoretical (associated with the prescription used). These results are obtained from a data sample that contains 657×10^6 $B\bar{B}$ pairs, collected near the $\Upsilon(4S)$ resonance with the Belle detector at the KEKB asymmetric energy e^+e^- collider. All results are preliminary.

PACS numbers: 13.30.Ce, 13.25.Hw, 14.40.Nd

I. INTRODUCTION

The Standard Model (SM) of particle physics contains a number of parameters whose values are not predicted by theory and must therefore be measured by experiment. In the quark sector, the elements of the Cabibbo-Kobayashi-Maskawa (CKM) matrix [1] govern the weak transitions between quark flavours, and precision measurements of their values are desirable. In particular, much experimental and theoretical effort is currently being employed to test the consistency of the Unitarity Triangle relevant to the decays of B mesons, which arises from the CKM formalism.

The angle $\sin 2\phi_1$, characterising indirect CP violation in $b \rightarrow \bar{c}s$ transitions, is now known to a precision of less than 4% [2]. This makes a precision measurement of the length of the side of the Unitarity triangle opposite to $\sin 2\phi_1$ particularly important as a consistency check of the SM picture. The length of this side is determined to good approximation by the ratio of the magnitudes of two CKM matrix elements, $|V_{ub}|/|V_{cb}|$. Both of these can be measured using exclusive semileptonic B meson decays. Using charmed semileptonic decays, the precision to which $|V_{cb}|$ has been determined is of order 1.5%. On the other hand $|V_{ub}|$, which can be measured using charmless semileptonic decays, is poorly known by comparison. Both inclusive and exclusive methods of measuring $|V_{ub}|$ have been pursued, with the inclusive methods giving values approaching 5% precision. The exclusive determination of $|V_{ub}|$ currently has a precision closer to 10%. It is the aim of an ongoing programme of measurements at the B factories to improve this precision to better than 5%, for comparison with the inclusive results, which have somewhat different experimental and theoretical systematics, and to provide a sharp consistency test with the value of $\sin 2\phi_1$.

Measurements of branching fractions for exclusive $B \rightarrow X_u \ell \nu$ decays, where X_u denotes a light meson containing a u quark, have been reported by the CLEO [3, 4, 5], BaBar [6, 7, 8, 9, 10, 11] and Belle [12, 13, 14] collaborations. A recent compilation of these results has been made by the Heavy Flavour Averaging Group (HFAG) [15]. In these measurements, three methods of identifying signal candidates have been employed, denoted “untagged”, “semileptonic tagged” or “full reconstruction tagged”.

The most precise measurements at the present time come from untagged analyses [5] [8]. As more integrated luminosity is accumulated by the B -factory experiments, full reconstruction tagging techniques to identify candidate B mesons, against which the signal B mesons recoil, will become the most precise method. These techniques hold the advantage of providing the best signal to background ratio, offset by the lowest efficiencies. In this paper we present preliminary studies of the exclusive semileptonic decays $B \rightarrow \pi^+ \ell \nu$, $B \rightarrow \pi^0 \ell \nu$, $B \rightarrow \rho^+ \ell \nu$, $B \rightarrow \rho^0 \ell \nu$ and $B \rightarrow \omega \ell \nu$ using such a full reconstruction tagging technique .

II. EXPERIMENTAL PROCEDURE

A. Data Sample and the Belle Detector

The data sample used for this analysis contains $657 \times 10^6 B\bar{B}$ pairs, collected with the Belle detector at the KEKB asymmetric-energy e^+e^- (3.5 on 8 GeV) collider [16]. KEKB operates at the $\Upsilon(4S)$ resonance ($\sqrt{s} = 10.58$ GeV) with a peak luminosity that exceeds $1.7 \times 10^{34} \text{ cm}^{-2}\text{s}^{-1}$. The $\Upsilon(4S)$ is produced with a Lorentz boost of $\beta\gamma = 0.425$ nearly along the electron beamline (z).

The Belle detector is a large-solid-angle magnetic spectrometer that consists of a silicon

vertex detector (SVD), a 50-layer central drift chamber (CDC), an array of aerogel threshold Cherenkov counters (ACC), a barrel-like arrangement of time-of-flight scintillation counters (TOF), and an electromagnetic calorimeter (ECL) comprised of CsI(Tl) crystals located inside a super-conducting solenoid coil that provides a 1.5 T magnetic field. An iron flux-return located outside of the coil is instrumented to detect K_L^0 mesons and to identify muons (KLM). The detector is described in detail elsewhere [17]. Two inner detector configurations were used. A 2.0 cm beampipe and a 3-layer silicon vertex detector was used for the first sample of $152 \times 10^6 B\bar{B}$ pairs, while a 1.5 cm beampipe, a 4-layer silicon detector and a small-cell inner drift chamber were used to record the remaining $505 \times 10^6 B\bar{B}$ pairs[18].

B. Full Reconstruction Tagging

In this analysis we fully reconstruct one of the two B mesons from the $\Upsilon(4S)$ decay (B_{tag}) in one of the following hadronic decay modes, $B^- \rightarrow D^{(*)0}\pi^-$, $B^- \rightarrow D^{(*)0}\rho^-$, $B^- \rightarrow D^{(*)0}a_1^-$, $B^- \rightarrow D^{(*)0}D_s^{*-}$, $\bar{B}^0 \rightarrow D^{(*)+}\pi^-$, $\bar{B}^0 \rightarrow D^{(*)+}\rho^-$, $\bar{B}^0 \rightarrow D^{(*)+}a_1^-$ or $\bar{B}^0 \rightarrow D^{(*)+}D_s^{*-}$. Within these B decay modes, the D mesons used in the reconstruction of B_{tag} are $D^0 \rightarrow K^-\pi^+$, $K^-\pi^+\pi^0$, $K^-\pi^+\pi^-\pi^+$, $K_S^0\pi^0$, $K_S^0\pi^+\pi^-$, $K_S^0\pi^+\pi^-\pi^0$ and K^+K^- , $D^+ \rightarrow K^-\pi^+\pi^+$, $K^-\pi^+\pi^+\pi^0$, $K_S^0\pi^+$, $K_S^0\pi^+\pi^0$, $K_S^0\pi^+\pi^+\pi^-$ and $K^+K^-\pi^+$, and $D_s^- \rightarrow K_S^0K^-$ and $K^+K^-\pi^-$. D^* mesons are reconstructed by combining a D candidate and a soft pion or photon [19].

The selection of B_{tag} candidates is based on the proximity of the beam-energy constrained mass $M_{\text{bc}} = \sqrt{E_{\text{beam}}^2 - P_B^2}$ and energy difference $\Delta E = E_B - E_{\text{beam}}$ to their nominal values of the B meson rest mass and zero, respectively. Here E_{beam} , P_B and E_B are the beam energy and the measured momentum and energy of the B_{tag} candidate in the $\Upsilon(4S)$ rest frame respectively. To be considered as a candidate, loose preselection conditions of $5.2 < M_{\text{bc}} < 5.3$ GeV and $-0.3 < \Delta E < 0.3$ GeV must be satisfied. If an event has multiple B_{tag} candidates, these are ordered according to a χ^2 variable based on ΔE , the D mass and the $D^* - D$ mass difference if appropriate. Following selection of the most likely B_{tag} candidate, events with B_{tag} satisfying the tighter selection criteria $M_{\text{bc}} > 5.27$ GeV and $-0.08 < \Delta E < 0.06$ GeV are retained.

C. Signal Reconstruction

Reconstructed charged tracks and ECL clusters which are not associated with the B_{tag} candidate are used to search for the signal B meson decays of interest recoiling against the B_{tag} . Photons identified with isolated ECL clusters which have a laboratory energy of less than 50 MeV are ignored. Electrons are identified using information on dE/dx from the CDC, response of the ACC, position matching between the reconstructed track and an ECL cluster, the ECL shower shape and the ratio of the energy deposited in the ECL to the momentum determined from tracking. The signals in the KLM are used to identify muons. Charged kaons are identified based on the dE/dx information from the CDC, the Cherenkov light yields in the ACC and time-of-flight information from the TOF counters. Any charged particles which are not identified as leptons or kaons are taken to be pions. Photons whose direction in the laboratory frame lies within a 5° cone of the direction of an identified electron or positron are considered to be bremsstrahlung. The 4-momentum of the photon is added to that of the lepton and the photon is not considered further.

Neutral pions are reconstructed from pairs of photons whose invariant mass lies in the range $[0.120, 0.150]$ GeV, of order $\pm 3\sigma$ of the π^0 mass. Charged ρ meson candidates are reconstructed via the decay $\rho^\pm \rightarrow \pi^\pm \pi^0$ where the invariant mass of the pair of pions is required to lie in the range $[0.570, 0.970]$ GeV. Neutral ρ meson candidates are similarly reconstructed from pairs of oppositely charged pions, with the requirement that $m_{\pi^+\pi^-}$ is in the range $[0.690, 0.850]$ GeV. Finally, ω candidates are reconstructed from $\omega \rightarrow \pi^+ \pi^- \pi^0$ with $m_{\pi^+\pi^-\pi^0}$ in the range $[0.703, 0.863]$ GeV. In events where more than one hadron candidate, denoted X_u , of a given type is identified amongst the recoil particles, the candidate with the highest momentum in the $\Upsilon(4S)$ rest frame is chosen.

To isolate signal candidates, several requirements are placed on the recoil system. There must be one lepton candidate present only. The total charge of the recoil system, Q_{recoil} , is required to be 0 if a neutral tag has been identified, and ± 1 if a charged tag has been identified. In the charged case, the sign of Q_{recoil} must be opposite to that of Q_{tag} . In the neutral case, we do not make any requirement on the sign of the lepton charge with respect to the B_{tag} , to allow for mixing.

The number of charged recoil particles is required to correspond to one of the sought signal modes, i.e. one for $B \rightarrow \pi^0 \ell \nu$ (the lepton), two for $B \rightarrow \pi^+ \ell \nu$ and $B \rightarrow \rho^+ \ell \nu$ (the lepton plus one charged pion) and three for $B \rightarrow \rho^0 \ell \nu$ and $B \rightarrow \omega \ell \nu$ (the lepton plus two charged pions). Additionally, the number of recoil π^0 candidates is required to be consistent with one of the sought modes. In order to increase efficiency, however, we allow more than the necessary number in some cases: we require no π^0 candidates to be present for $B \rightarrow \pi^+ \ell \nu$ and $B \rightarrow \rho^0 \ell \nu$ modes, and at least one π^0 for the $B \rightarrow \pi^0 \ell \nu$ and $B \rightarrow \rho^+ \ell \nu$ modes, and exactly one π^0 for the $B \rightarrow \omega \ell \nu$ mode. Additionally, we require that there be no more than 0.5 GeV of residual neutral energy present on the recoil side, calculated in the $\Upsilon(4S)$ rest frame, after any photons contributing to the X_u candidate have been removed.

If the tagging B is correctly reconstructed and the correct lepton and hadron candidate have been identified on the recoil side, then ideally all missing 4-momentum is due to the remaining unidentified neutrino. Signal events can therefore be identified by examining the missing mass squared (M_{miss}^2), defined to be the square of the missing 4-momentum. In signal events this quantity should be close to zero, and applying this requirement provides a very strong discrimination between signal and background. In practice we construct the recoiling B meson to have its nominal energy and magnitude of momentum in the $\Upsilon(4S)$ rest frame, and direction opposite to B_{tag} . The missing 4-momentum vector of the decaying recoil B system is then obtained by subtracting the 4-momenta of the hadron candidate and lepton from the B 4-momentum.

For signal candidates, the neutrino 4-momentum is defined to be $p_\nu = (|\vec{p}_{\text{miss}}|, \vec{p}_{\text{miss}})$, where \vec{p}_{miss} is the missing 3-momentum vector of the recoil B system defined as above. The kinematical variable q^2 , defined to be the invariant mass squared of the lepton-neutrino system, can then be determined. The q^2 resolution obtained using this procedure is excellent, varying from 0.21 GeV² for the $B \rightarrow \pi^+ \ell \nu$ channel to 0.28 GeV² for the $B \rightarrow \omega \ell \nu$ channel.

D. Background Estimation

Background contributions come from several sources. These include semileptonic decays resulting from $b \rightarrow c \ell \nu$ transitions, denoted $B \rightarrow X_c \ell \nu$, which have significantly larger branching fractions than the channels under study; continuum $e^+ + e^- \rightarrow q\bar{q}$ processes; and cross feed from one $B \rightarrow X_u \ell \nu$ channel into another. The contributions of these backgrounds

are studied using Monte Carlo (MC) simulated data samples generated with the EvtGen package [20]. Generic $B\bar{B}$ and continuum MC samples equivalent to approximately three times the integrated luminosity of the real data set are used. The model adopted for $B \rightarrow D^*\ell\nu$ and $B \rightarrow D\ell\nu$ decays is based on HQET and parametrisation of the form factors [21], while $B \rightarrow D^{**}\ell\nu$ decays are based on the ISGW2 model [22]. A non-resonant $B \rightarrow D^{(*)}\pi\ell\nu$ component based on the Goity-Roberts prescription [23] is also included.

A separate MC sample equivalent to approximately sixteen times the integrated luminosity of the real data set is used to simulate the signal channels and crossfeed from other $B \rightarrow X_u\ell\nu$ decays. Models for the exclusive modes are based on Light Cone Sum Rules (LCSR) for π [24], ρ and ω [25] modes and ISGW2 [22] for other exclusive modes.

Radiative effects associated with the lepton and resulting from higher-order QED processes are modelled in all MC samples using the PHOTOS package [26]. All generated MC events are passed through a full simulation of Belle detector effects based on GEANT 3.21 [27].

III. RESULTS AND SYSTEMATIC UNCERTAINTIES

A. Signal yield determination

In order to obtain the signal yields, a fit is performed to the observed M_{miss}^2 distributions, individually for each mode. The fits are made in three separate bins of q^2 in order to obtain the yields as a function of q^2 , and to minimise the systematic error which arises from the lack of precise knowledge of the shape of the form factors in $B \rightarrow X_u\ell\nu$ decays. The q^2 bins are chosen commensurate with available statistics, and are 0 to 8 GeV², 8 to 16 GeV², and greater than 16 GeV². The components of any given fit are signal, $u\ell\nu$ crossfeed and the contribution from other backgrounds, which is dominated by $B \rightarrow X_c\ell\nu$ decays. The shapes of the components are taken from MC and the normalizations are fit parameters. The fitting method follows that of Barlow and Beeston [28] and takes into account finite MC statistics. In Fig. 1 the observed M_{miss}^2 distributions for the five decay modes are shown, summed over the three q^2 bins. The fit components shown in the figures are likewise those obtained by summing the results of the fits in the individual q^2 bins. The fitted event yields obtained in this way are 59 ± 10 for the $B \rightarrow \pi^+\ell\nu$ mode, 49 ± 9 for $B \rightarrow \pi^0\ell\nu$, 65 ± 12 for $B \rightarrow \rho^+\ell\nu$, 80 ± 10 for $B \rightarrow \rho^0\ell\nu$ and 25 ± 8 for $B \rightarrow \omega\ell\nu$.

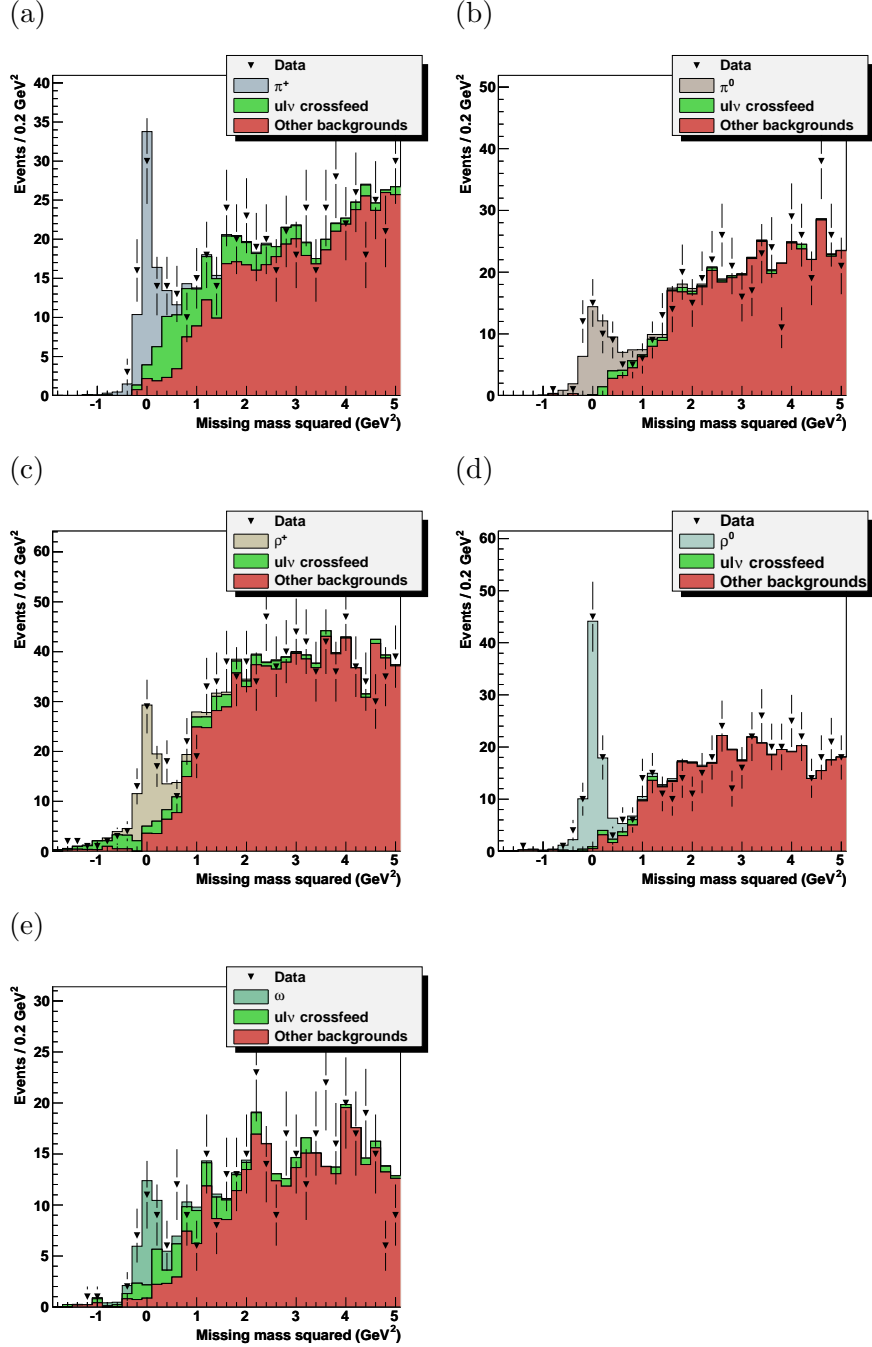
B. Branching Fractions

We extract the partial branching fractions in bins of q^2 , using the formula

$$\Delta\mathcal{B}(B \rightarrow X_u\ell\nu) = \frac{\text{Signal Yield}}{\epsilon \cdot 2N_{B\bar{B}}}$$

where ϵ is the signal efficiency within the M_{miss}^2 range corresponding to the histograms in Fig. 1, and $N_{B\bar{B}}$ is the number of $B\bar{B}$ pairs which the data set is estimated to contain before any event selections are made. The signal efficiencies are estimated from MC and do not exhibit a strong q^2 dependence. Averaged over q^2 , these efficiencies are $(0.0401 \pm 0.0012)\%$ for the $B \rightarrow \pi^+\ell\nu$ mode, $(0.0581 \pm 0.0020)\%$ for $B \rightarrow \pi^0\ell\nu$, $(0.0196 \pm 0.0006)\%$ for $B \rightarrow \rho^+\ell\nu$,

FIG. 1: Missing mass squared (M_{miss}^2) distributions after all selection criteria, for (a) $B \rightarrow \pi^+ \ell \nu$, (b) $B \rightarrow \pi^0 \ell \nu$, (c) $B \rightarrow \rho^+ \ell \nu$, (d) $B \rightarrow \rho^0 \ell \nu$, and (e) $B \rightarrow \omega \ell \nu$ modes. Data is indicated by the points with error bars. The signal histogram (lightest shade in greyscale in each case) shows the fitted prediction based on the LCSR model [24, 25]. The green histogram (middle shade in greyscale) shows the fitted $b \rightarrow u \ell \nu$ background contribution. The crimson histogram (darkest shade in greyscale) shows the fitted background contribution from other sources. The fitting method is explained in the text.



$(0.0339 \pm 0.0010)\%$ for $B \rightarrow \rho^0 l \nu$ and $(0.0172 \pm 0.0007)\%$ for $B \rightarrow \omega l \nu$. The number of $B\bar{B}$ pairs is $(656.6 \pm 8.9) \times 10^6$.

The resultant partial branching fractions are given in Table I. The first error given in each case is statistical, and the second systematic, as described in the following section. Figure 2 presents the shapes of the partial branching fractions for all five modes as a function of q^2 , where the error bars displayed are obtained by adding the statistical and systematic errors in quadrature. Also shown in this figure are the predictions based on LCSR prescriptions [24, 25] and a quark model prescription [22]. The predictions are normalised to have the same area as that of the data distribution in each case. For the pion decay modes in particular it is clear that the LCSR prescription is in better agreement with the data.

TABLE I: Partial branching fractions in three bins of q^2 . These are summed to give the full branching fraction quoted in the ‘‘Sum’’ column. Errors are statistical and systematic.

Mode	$\Delta\mathcal{B} [10^{-4}]$			$\mathcal{B} [10^{-4}]$
	$0 < q^2 < 8$ (GeV ²)	$8 < q^2 < 16$ (GeV ²)	$q^2 > 16$ (GeV ²)	Sum (GeV ²)
$B \rightarrow \pi^+ l \nu$	$0.43 \pm 0.11 \pm 0.02$	$0.42 \pm 0.11 \pm 0.02$	$0.26 \pm 0.08 \pm 0.01$	$1.12 \pm 0.18 \pm 0.05$
$B \rightarrow \pi^0 l \nu$	$0.26 \pm 0.09 \pm 0.01$	$0.17 \pm 0.05 \pm 0.01$	$0.22 \pm 0.06 \pm 0.01$	$0.66 \pm 0.12 \pm 0.03$
$B \rightarrow \rho^+ l \nu$	$0.74 \pm 0.29 \pm 0.04$	$1.01 \pm 0.28 \pm 0.05$	$0.81 \pm 0.21 \pm 0.04$	$2.56 \pm 0.46 \pm 0.12$
$B \rightarrow \rho^0 l \nu$	$0.72 \pm 0.15 \pm 0.03$	$0.70 \pm 0.13 \pm 0.03$	$0.39 \pm 0.11 \pm 0.02$	$1.80 \pm 0.23 \pm 0.07$
$B \rightarrow \omega l \nu$	$0.23 \pm 0.17 \pm 0.01$	$0.64 \pm 0.21 \pm 0.03$	$0.32 \pm 0.17 \pm 0.01$	$1.19 \pm 0.32 \pm 0.05$

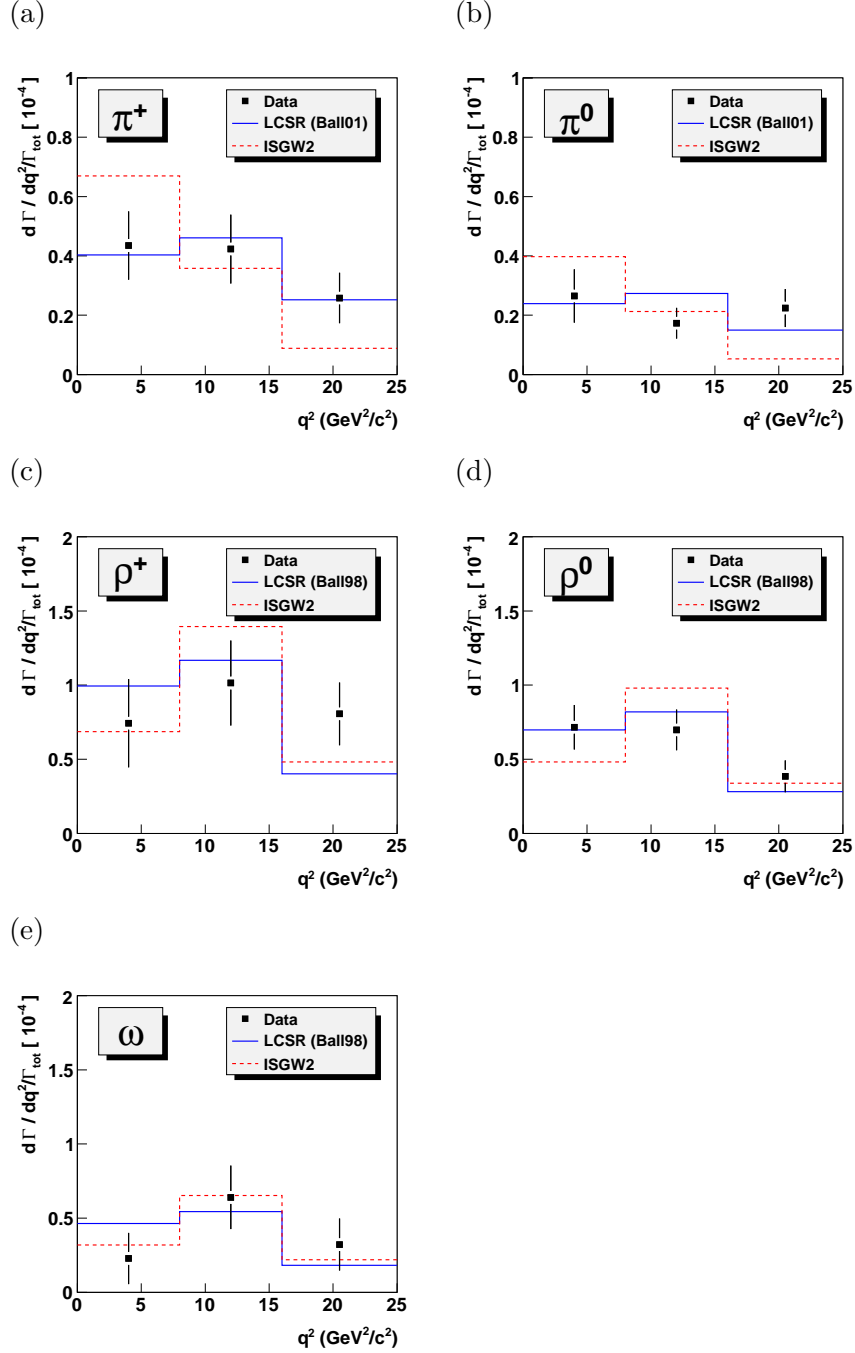
C. Systematic Uncertainties

Table II summarises the preliminary result of a study of the contributions to the total systematic error for the branching fractions summed over the three q^2 bins, for each of the $B \rightarrow X_u l \nu$ signal modes. These are broken down into the following categories; those arising from detector simulation, such as charged track reconstruction efficiency, particle identification and neutral cluster reconstruction; uncertainties in the luminosity; and effects of the form factor models used and assumed branching fractions in the MC.

The detector simulation errors have been obtained following the procedure described in a Belle study of similar final states in reference [13]. The effects of model dependence of the form factor shapes assumed in the $B \rightarrow X_u l \nu$ MC used for signal efficiency and crossfeed background estimates have been studied by comparing the fitted yields obtained using the default model implemented in the MC, which is LCSR [24, 25], and the ISGW2 model [22]. This is achieved by reweighting the MC events on an event-by-event basis based on their generated values of q^2 and angular variables. The variation between these two models in predicting the shapes of the q^2 distributions for the pseudoscalar and vector modes typifies the spread between available models for the dynamics of these decays.

The shapes of the background M_{miss}^2 components used in the fits can be affected by the assumed branching fractions of dominantly contributing $b \rightarrow ul\nu$ and $b \rightarrow cl\nu$ decays in

FIG. 2: Partial branching fractions as a function of q^2 for the five signal modes (a) $B \rightarrow \pi^+ \ell \nu$, (b) $B \rightarrow \pi^0 \ell \nu$, (c) $B \rightarrow \rho^+ \ell \nu$, (d) $B \rightarrow \rho^0 \ell \nu$, and (e) $B \rightarrow \omega \ell \nu$. Errors shown are statistical and preliminary systematic, added in quadrature. LCSR predictions [24, 25] are shown in blue (solid line) and a quark model prediction [22] in red (dashed line). The predictions are normalised to have the same area as that of the data distribution in each case.



the MC samples used. This was studied by varying in turn the $B \rightarrow \pi^+\ell\nu$, $B \rightarrow \pi^0\ell\nu$, $B \rightarrow \rho^+\ell\nu$, $B \rightarrow \rho^0\ell\nu$, $B \rightarrow \omega\ell\nu$, $B \rightarrow D^+\ell\nu$, $B \rightarrow D^0\ell\nu$, $B \rightarrow D^{*+}\ell\nu$ and $B \rightarrow D^{*0}\ell\nu$ branching fractions by their measurement errors as quoted by the Particle Data Group [29]. A reweighting technique is again used, and fitted yields with and without reweighting are compared. The maximum observed spread in the fitted branching fraction is assigned as systematic error.

The effects of finite MC statistics are taken into account in the fitting procedure [28] and are reflected in the errors on the obtained branching fractions. Since the available MC samples are rather limited in statistics, variations of the assumptions on form factor shapes and normalizations can be absorbed by the present fits to a significant extent.

TABLE II: Preliminary results of a study of sources of systematic uncertainty.

Source of error	Assigned systematic error				
	$B \rightarrow \pi^+\ell\nu$	$B \rightarrow \pi^0\ell\nu$	$B \rightarrow \rho^+\ell\nu$	$B \rightarrow \rho^0\ell\nu$	$B \rightarrow \omega\ell\nu$
Detector Simulation:					
Pion track finding eff.	1.0%	-	1.0%	2.0%	2.0%
π^0 reconstruction eff.	-	2.0%	2.0%	-	2.0%
Lepton track finding eff.	1%	1%	1%	1%	1%
Lepton identification	2.1%	2.1%	2.1%	2.1%	2.1%
Pion identification	2.0%	2.0%	2.0%	2.0%	2.0%
Combined	3.2%	3.7%	3.8%	3.7%	4.2%
$N(B\bar{B})$ uncertainty	1.36%	1.36%	1.36%	1.36%	1.36%
Form Factor Shapes:					
π (LCSR \rightarrow ISGW2)	1.5%	0.0%	1.0%	0.0%	0.0%
ρ, ω (LCSR \rightarrow ISGW2)	1.8%	0.5%	2.2%	0.1%	0.2%
Branching Fractions:					
$b \rightarrow u\ell\nu/b \rightarrow c\ell\nu$ norm.	0.3%	0.2%	1.1%	0.6%	0.5%
Total systematic error	4.2%	3.9%	4.8%	4.0%	4.4%

D. Fully reconstructed charmed semileptonic decays

In order to check the robustness of our method, we apply it to exclusive $B \rightarrow X_c\ell\nu$ modes, where the branching fractions are larger and better known than in the $B \rightarrow X_u\ell\nu$ case. We use the channels $B \rightarrow D^+\ell\nu$, $B \rightarrow D^0\ell\nu$, $B \rightarrow D^{*+}\ell\nu$ and $B \rightarrow D^{*0}\ell\nu$, applying a similar method to that used for the $B \rightarrow X_u\ell\nu$ modes. The decay channels of the charmed mesons used are $D^+ \rightarrow K^-\pi^+\pi^+$, $D^0 \rightarrow K^-\pi^+$, $D^{*+} \rightarrow D^0\pi^+$, $D^{*+} \rightarrow D^+\pi^0$, $D^{*0} \rightarrow D^0\pi^0$ and $D^{*0} \rightarrow D^0\gamma$. The mass windows used in selecting the charmed meson are set to be [1.67, 2.07] GeV for D^+ , [1.84, 1.89] GeV for D^0 , [1.95, 2.25] GeV for D^{*+} and [1.99, 2.03] GeV for D^{*0} . Particle identification used is the same as for the $B \rightarrow X_u\ell\nu$ modes. The range of q^2 for charmed semileptonic decays is more narrow than for the

charmless case, and we break the range into the following three bins of q^2 : $0 < q^2 < 3 \text{ GeV}^2$, $3 < q^2 < 6 \text{ GeV}^2$ and $6 < q^2 < 16 \text{ GeV}^2$.

In performing the fits to the charm modes, the crossfeed components used depend on the signal channel. For the $B \rightarrow D^+\ell\nu$ channel the background is divided into a $B \rightarrow D^{*+}\ell\nu$ component and all other backgrounds combined; for the $B \rightarrow D^0\ell\nu$ channel the crossfeed component is $B \rightarrow D^{*0}\ell\nu$; for $B \rightarrow D^{*+}\ell\nu$ the crossfeed component is $B \rightarrow D^+\ell\nu$; and for $B \rightarrow D^{*0}\ell\nu$ the crossfeed component is $B \rightarrow D^0\ell\nu$. Following the same method employed for the charmless signal modes, the partial branching fractions are extracted in each q^2 bin and summed to give the total branching fraction. The results are shown in Table III, where they are compared to the current PDG values [29]. The agreement is excellent.

TABLE III: Branching fractions for charm modes obtained from fitting in 3 q^2 bins and then summing the partial branching fractions, compared to Particle Data Group values. Errors in the ‘‘Fitted’’ column are statistical only, but take into account the finite MC statistics.

Mode	Fitted \mathcal{B} [%]	PDG \mathcal{B} [%]
$B \rightarrow D^+\ell\nu$	2.05 ± 0.18	2.08 ± 0.18
$B \rightarrow D^0\ell\nu$	2.07 ± 0.17	2.15 ± 0.22
$B \rightarrow D^{*+}\ell\nu$	4.91 ± 0.48	5.29 ± 0.19
$B \rightarrow D^{*0}\ell\nu$	5.16 ± 0.41	6.5 ± 0.5

E. Determination of $|V_{ub}|$

The CKM matrix parameter $|V_{ub}|$ may be extracted from the partial branching fraction $\Delta\mathcal{B}$ for $B \rightarrow \pi^+\ell\nu$ decay using the formula $|V_{ub}| = \sqrt{\Delta\mathcal{B}/(\tau_{B^0}\Delta\zeta)}$, where $\tau_{B^0} = (1.530 \pm 0.009) \text{ ps}$ [29] and $\Delta\zeta = \Delta\Gamma/|V_{ub}|^2$ is the normalised partial decay rate predicted from theoretical form factor calculations.

For $\Delta\zeta$ we take the values predicted from two approaches, a LCSR calculation appropriate to the kinematic region $q^2 < 16 \text{ GeV}^2$ [30] and recent Lattice QCD calculations valid for $q^2 > 16 \text{ GeV}^2$ [31, 32].

We can improve the precision of our determination of $|V_{ub}|$ by assuming that isospin symmetry is valid and combining the measurements of the charged and neutral pion modes. To achieve this, the branching fraction for the neutral pion mode in each bin of q^2 is first multiplied by a factor $2 * \tau_{B^0}/\tau_{B^+}$ to account for the difference in charged and neutral B meson lifetimes, using $\tau_{B^+}/\tau_{B^0} = 1.071 \pm 0.009$ [29]. A weighted average of this corrected $B \rightarrow \pi^0\ell\nu$ branching fraction and the $B \rightarrow \pi^+\ell\nu$ branching fraction is then formed, using weights $1/\sigma_i^2$ where σ_i is the statistical error on the partial branching fraction $i = \pi^+, \pi^0$. The systematic error is taken as the weighted average of the individual systematic errors, using the same weights. The resultant branching fraction obtained over the full q^2 region is

$$\mathcal{B}(B \rightarrow \pi\ell\nu)_{\text{all } q^2} = (1.13 \pm 0.14 \pm 0.06) \times 10^{-4}$$

and the partial branching fractions obtained in the low and high q^2 ranges relevant to $|V_{ub}|$ determination are

$$\Delta\mathcal{B}(B \rightarrow \pi\ell\nu)_{q^2 < 16 \text{ GeV}^2} = (0.82 \pm 0.12 \pm 0.04) \times 10^{-4}$$

$$\Delta\mathcal{B}(B \rightarrow \pi\ell\nu)_{q^2 > 16 \text{ GeV}^2} = (0.31 \pm 0.07 \pm 0.02) \times 10^{-4}$$

respectively.

The results of the $|V_{ub}|$ determination are displayed in Table IV, both for the case when the $B \rightarrow \pi^+\ell\nu$ partial branching fractions are used, and when the above combined $B \rightarrow \pi^+\ell\nu$ and $B \rightarrow \pi^0\ell\nu$ partial branching fractions are used.

TABLE IV: Values of $|V_{ub}|$ extracted from the measured $B \rightarrow \pi^+\ell\nu$ partial branching fractions and from the combined $B \rightarrow \pi^+\ell\nu$ and $B \rightarrow \pi^0\ell\nu$ partial branching fractions. The first error is statistical, the second systematic, and the third due to the theoretical errors quoted for the form-factor calculations.

	Mode	q^2 [GeV ²]	$\Delta\zeta$ [ps ⁻¹]	$ V_{ub} $ [10^{-3}]
Ball-Zwicky [30]	π^+	< 16	5.44 ± 1.43	$3.2 \pm 0.3 \pm 0.1^{+0.5}_{-0.4}$
Gulez et. al. [31]	π^+	> 16	2.07 ± 0.57	$2.9 \pm 0.5 \pm 0.1^{+0.5}_{-0.3}$
Okamoto et. al. [32]	π^+	> 16	1.83 ± 0.50	$3.0 \pm 0.5 \pm 0.1^{+0.5}_{-0.3}$
Ball-Zwicky [30]	$\pi^+ + \pi^0$	< 16	5.44 ± 1.43	$3.1 \pm 0.2 \pm 0.1^{+0.5}_{-0.3}$
Gulez et. al. [31]	$\pi^+ + \pi^0$	> 16	2.07 ± 0.57	$3.1 \pm 0.3 \pm 0.1^{+0.6}_{-0.4}$
Okamoto et. al. [32]	$\pi^+ + \pi^0$	> 16	1.83 ± 0.50	$3.3 \pm 0.4 \pm 0.1^{+0.6}_{-0.4}$

IV. SUMMARY

In summary, we have made a study of the partial branching fractions as a function of q^2 for five semileptonic decay channels of B mesons to charmless final states, using a full reconstruction tag method. Summed over the three q^2 bins we obtain the following estimates of the branching fractions: $\mathcal{B}(B \rightarrow \pi^+\ell\nu) = (1.12 \pm 0.18 \pm 0.05) \times 10^{-4}$, $\mathcal{B}(B \rightarrow \pi^0\ell\nu) = (0.66 \pm 0.12 \pm 0.03) \times 10^{-4}$, $\mathcal{B}(B \rightarrow \rho^+\ell\nu) = (2.56 \pm 0.46 \pm 0.12) \times 10^{-4}$, $\mathcal{B}(B \rightarrow \rho^0\ell\nu) = (1.80 \pm 0.23 \pm 0.07) \times 10^{-4}$, $\mathcal{B}(B \rightarrow \omega\ell\nu) = (1.19 \pm 0.32 \pm 0.05) \times 10^{-4}$, where the first error is statistical and the second systematic. From these branching fractions and theoretical form factor calculations, values for $|V_{ub}|$ have been obtained. All results are preliminary.

Whilst the statistical precision of these measurements is limited at present, the potential power of the full reconstruction tagging method, when it can be used with larger accumulated B -factory data samples in the future, can clearly be seen.

Acknowledgments

We thank the KEKB group for the excellent operation of the accelerator, the KEK cryogenics group for the efficient operation of the solenoid, and the KEK computer group and the National Institute of Informatics for valuable computing and SINET3 network support. We acknowledge support from the Ministry of Education, Culture, Sports, Science, and

Technology of Japan and the Japan Society for the Promotion of Science; the Australian Research Council and the Australian Department of Education, Science and Training; the National Natural Science Foundation of China under contract No. 10575109 and 10775142; the Department of Science and Technology of India; the BK21 program of the Ministry of Education of Korea, the CHEP SRC program and Basic Research program (grant No. R01-2005-000-10089-0) of the Korea Science and Engineering Foundation, and the Pure Basic Research Group program of the Korea Research Foundation; the Polish State Committee for Scientific Research; the Ministry of Education and Science of the Russian Federation and the Russian Federal Agency for Atomic Energy; the Slovenian Research Agency; the Swiss National Science Foundation; the National Science Council and the Ministry of Education of Taiwan; and the U.S. Department of Energy.

-
- [1] N. Cabibbo, Phys. Rev. Lett. **10**, 531 (1963). M. Kobayashi and T. Maskawa, Prog. Theor. Phys. **49**, 652 (1973).
 - [2] For a recent review presented at FPCP08 see K. Vervink, arXiv:0807.0496 [hep-ex].
 - [3] B. H. Behrens *et al.* (CLEO Collab.), Phys. Rev. D **61**, 052001 (2000) [arXiv:hep-ex/9905056].
 - [4] S. B. Athar *et al.* (CLEO Collab.), Phys. Rev. D **68**, 072003 (2003) [arXiv:hep-ex/0304019].
 - [5] N. Adam *et al.* (CLEO Collab.), Phys. Rev. Lett. **99**, 041802 (2007) [arXiv:hep-ex/0703041v2].
 - [6] B. Aubert *et al.* (BaBar Collab.), Phys. Rev. Lett. **90**, 181801 (2003) [arXiv:hep-ex/0301001v1].
 - [7] B. Aubert *et al.* (BaBar Collab.), Phys. Rev. D **72**, 051102 (2005) [arXiv:hep-ex/0507003].
 - [8] B. Aubert *et al.* (BaBar Collab.), Phys. Rev. Lett. **98**, 091801 (2007) [arXiv:hep-ex/0612020].
 - [9] B. Aubert *et al.* (BaBar Collab.) arXiv:0805.2408 [hep-ex].
 - [10] B. Aubert *et al.* (BaBar Collab.), Phys. Rev. Lett. **97** 211801 (2006) [arXiv:hep-ex/0607089].
 - [11] B. Aubert *et al.* (BaBar Collab.) [arXiv:hep-ex/0607066v1].
 - [12] C. Schwanda *et al.* (Belle Collab.), Phys. Rev. Lett. **93**, 131803 (2004) [arXiv:hep-ex/0402023v2].
 - [13] T. Hokuue *et al.* (Belle Collab.), Phys. Lett. B **648**, 139 (2007) [arXiv:hep-ex/0604024].
 - [14] K. Abe *et al.* (Belle Collab.) arXiv:hep-ex/0610054.
 - [15] Heavy Flavor Averaging Group, <http://www.slac.stanford.edu/xorg/hfag> .
 - [16] S. Kurokawa and E. Kikutani, Nucl. Instr. and Meth. A **499**, 1 (2003), and other papers included in this volume.
 - [17] A. Abashian *et al.* (Belle Collab.), Nucl. Instr. and Meth. A **479**, 117 (2002).
 - [18] Y. Ushiroda (Belle SVD2 Group), Nucl. Instr. and Meth. A **511** 6 (2003).
Z. Natkaniec *et al.*, Nucl. Instr. and Meth. A **560** 1 (2006).
 - [19] Throughout this paper, the inclusion of the charge conjugate mode decay is implied unless otherwise stated.
 - [20] D.J. Lange, Nucl. Instrum. Meth. A **462**, 152 (2001).
 - [21] I. Caprini, L. Lellouch and M. Neubert, Nucl. Phys. B **530**, 153 (1998).
 - [22] D. Scora and N. Isgur, Phys. Rev. D **52**, 2783 (1995).
 - [23] J.L. Goity and W. Roberts, Phys. Rev. D **51**, 3459 (1995).
 - [24] P. Ball and R. Zwicky, JHEP **0110**, 19 (2001).
 - [25] P. Ball and V. M. Braun, Phys. Rev. D **58**, 094016 (1998).
 - [26] E. Barberio and Z. Was, Comp. Phys. Commun. **79**, 291 (1994).

- [27] R. Brun *et al.* GEANT 3.21 CERN Report DD/EE/84-1, (1984).
- [28] R. Barlow and C. Beeston, *Comp. Phys. Comm.* **77**, 219 (1993).
- [29] W.-M. Yao *et al.* (Particle Data Group), *J. Phys. G* **33**, 1 (2006).
- [30] P. Ball and R. Zwicky, *Phys. Rev. D* **71**, 014015 (2005).
- [31] HPQCD Collaboration, E. Gulez *et al.*, *Phys. Rev. D* **73**, 074502 (2006), [arXiv:hep-lat/0601201]. Erratum *Phys. Rev. D* **75**, 119906(E) (2007).
- [32] FNAL Collaboration, M. Okamoto *et al.*, *Nucl. Phys. Proc. Suppl.* **140**, 461 (2005) [arXiv:hep-lat/0409116].